HRCT Features Between Lepidic-Predominant Type and Other Pathological Subtypes in Early-Stage Invasive Pulmonary Adenocarcinoma Appearing as a Ground-Glass Nodule

Pengju Zhang
Fourth Medical Center of PLA General Hospital
Tianran Li
Fourth Medical Center of PLA General Hospital
Xuemin Tao
First Medical Center of PLA General Hospitall
Xin Jin
First Medical Center of PLA General Hospital
Shaohong Zhao (zhaoshaohong@aliyun.com)
First Medical Center of PLA General Hospital

Research article

Keywords: Lung neoplasms, Ground glass nodule, Tomography, X-ray computed, Pathology

Posted Date: April 5th, 2021

DOI: https://doi.org/10.21203/rs.3.rs-386984/v1

Abstract

Background: We aimed to investigate the high-resolution computed tomography (HRCT) features of lepidic-predominant type and other pathological subtypes of early-stage (T1N0M0) invasive pulmonary adenocarcinoma appearing as a ground-glass nodule (GGN).

Methods: We performed a retrospective analysis on clinical data and HRCT features of 630 lesions in 589 patients with pathologically confirmed invasive pulmonary adenocarcinomas presenting as pure GGN and mixed GGN [consolidation-to-tumor ratio (CTR), <0.5] from January to December 2019. All GGNs were classified as lepidic-predominant adenocarcinoma (LPA) and nonlepidic-predominant adenocarcinoma (n-LPA) groups. Univariate analysis was performed to analyze the difference of clinical data and HRCT features between the LPA and n-LPA groups. Multivariate analysis was conducted to determine the variables to distinguish the LPA from n-LPA group independently. The diagnostic performance of different parameters was compared using receiver operating characteristic curves.

Results: In total, 367 GGNs in the LPA group and 263 GGNs in the n-LPA group were identified. In the univariate analysis, the CTR, mean computed tomography (CT) values, and mean diameters as well as mixed GGN, deep lobulation, spiculation, vascular change, bronchial change, and tumor–lung interface were smaller in the LPA group than in the n-LPA group ($P < 0.05$). Logistic regression model was reconstructed including the mean CT value, deep lobulation, and vascular change ($P < 0.001$), as well as CTR, spiculation, and bronchial change ($P < 0.05$). Area under the curve of the logistic regression model for differentiating LPA and n-LPA was 0.840 (76.4% sensitivity, 78.7% specificity), which was significantly higher than that of the mean CT value or CTR (both $P < 0.05$).

Conclusions: HRCT features were helpful in differentiating lepidic-predominant type from other subtypes in early-stage GGN invasive pulmonary adenocarcinoma. The mean CT value of <−472.5 HU and CTR of <27.4% were highly suspected in lepidic-predominant invasive pulmonary adenocarcinoma.

Background

With the development and popularization of high-resolution computed tomography (HRCT) lung cancer screening, the detection rate of ground-glass nodule (GGN) has significantly increased. Numerous studies have confirmed that most long-term existed GGN in the lung is mostly early lung adenocarcinoma or its precancerous lesions [1–4]. According to the 2017 Fleischner Society Guidelines [5], GGN can be classified as pure ground-glass nodule (pGGN), mixed ground-glass nodule (mGGN), or part-solid nodule (PSN); PSN is further classified as ground-glass–predominant nodules [0 < consolidation-to-tumor ratio (CTR) < 0.5] and consolidation-predominant nodules ($0.5 \leq CTR < 1$) according to CTR. Matsunaga et al. [6] found that lymphatic invasion was lower and the 5-year recurrence-free survival rate was better in ground-glass–predominant nodules than in consolidation-predominant nodules.

The 2015 World Health Organization (WHO) Classification of Lung Tumors [7] classified invasive pulmonary adenocarcinoma (IPA) into lepidic, acinar, papillary, micropapillary, solid subtypes according

to the main growth patterns. Among them, lepidic-predominant adenocarcinoma has the best prognosis, followed by the acinar and papillary types, whereas solid and micropapillary types have the worst [8, 9]. Furthermore, different pathological subtypes of early-stage GGN IPA have different clinical treatment methods and options [10–12]. Early-stage lepidic-predominant IPA can be treated with segmentectomy + lymph node sampling/dissection, whereas other types can be treated with standard therapy for anatomical lobectomy + lymph node sampling/dissection. Surgeons should more carefully choose the surgery and surgical methods considering the patient's age, lung function, medical history, and other factors. Although a previous study [13] has shown that the ground-glass component on HRCT is positively correlated with the lepidic growth pattern of the tumor pathologically, different pathological IPA subtypes can be expressed as pGGN and mGGN [14]. Our previous studies also showed that even with pGGN, 39% are IPAs [15]. Therefore, HRCT features should be used to identify lepidic-predominant IPA in GGN, which can help clinicians to decide the surgical method. However, previous reports mainly focused on the imaging comparison between preinvasive and invasive lesions [16, 17], and analyses of imaging among IPA subtypes are limited.

In this study, the HRCT features of GGN IPA were retrospectively analyzed to determine imaging differences between the lepidic-predominant IPA and other pathological subtypes to provide imaging help for clinical surgical decision-making.

Materials And Methods

This study was approved by the Ethics Committee of Fourth Medical Center of Chinese PLA General Hospital (approval No. 2019YL002-HS001). All participants and/or their family members provided the informed consent.

Participants

The clinical and CT imaging data of patients having a confirmed diagnosis of IPA based on pathological results and undergoing resection at the Department of Thoracic Surgery of our hospital from January to December 2019 were collected. The inclusion criteria were as follows: (1) confirmed diagnosis of early-stage (T1N0M0) invasive lung adenocarcinoma (without variants); (2) preoperative CT images appearing as GGN; and (3) no radiotherapy, chemotherapy, or CT-guided percutaneous biopsy performed before the CT examination. The exclusion criteria were as follows: (1) no routine CT examination or 1–1.25-mm thin-slice imaging performed within 1 month preoperatively; (2) heavy respiratory artifacts; (3) GGN with a maximum diameter of > 3 cm or CTR of ≥ 0.5 on CT; (4) GGN with air space type, affecting the measurement of the CT value. Finally, 589 patients (630 GGNs in total) were included for analysis (Fig. 1). Multiple GGNs in the lung were analyzed as independent lesions.

A total of 630 GGN IPAs were divided into lepidic-predominant adenocarcinoma (LPA) and nonlepidic-predominant adenocarcinoma (n-LPA) groups. The LPA group included lepidic-predominant IPA, whereas the n-LPA group included acinar-, papillary-, micropapillary-, and solid-predominant types. The 2015 WHO

Classification of Lung Tumors classified invasive adenocarcinoma according to the main growth mode of the tumor and semiquantitatively evaluated the proportion of various growth modes in 5% increments. As a small number of micropapillary structures in IPA are strongly associated with poor prognosis, GGN with micropapillary structure is classified as micropapillary type [7].One attending physician screened the participants and recorded the relevant clinical data.

Inspection method

Brilliance iCT256 CT scanner (Philips Medical Systems, Netherland) or GE Optima 64 spiral CT scanner (GE Healthcare Technologies, Waukesha, WI) was used for conventional chest CT volume scanning. The scanning range was from the lung apex to the posterior costophrenic angle. The CT scan parameters were as follows: tube voltage, 120 kV; pitch, 0.993; matrix, 768 × 768; scanning slice thickness, 5 mm; reconstruction slice thickness, 1 or 1.25 mm; use of bone and standard algorithms; lung window (window width, 1,500 HU and window level, -600 HU); and mediastinal window (window width, 400 HU and window level, 40 HU).

Analysis of clinical data and HRCT features

Clinical data were collected from the thoracic surgery database of our hospital, including patient's age, sex, smoking history, and surgical records.

The HRCT features of GGN, including location, type, deep lobulation, spiculation, vascular change, bronchial change, bubble-like lucency, pleural indentation sign, tumor–lung interface, mean diameter, CTR, and mean CT value, were browsed and analyzed on the Picture Archiving & Communication System. The types of nodules included pGGN and mGGN. Deep lobulation is characterized as a scallop-like lobulation on the nodule surface, and the maximum single lobulation chord distance/chord length is ≥ 0.4. Vascular change refers to the dilation, stiffness, distortion, and aggregation of blood vessels in GGN. Bronchial change refers to dilation, distortion, and truncation in nodules. The tumor–lung interface is a clear or fuzzy boundary between the tumor and adjacent normal lung tissue. The mean diameter refers to the mean value of the longest diameter (D_{max}) of the nodule measured at the maximum level of the lung window and the maximum short diameter (D_{per}) perpendicular to it. The calculation method is as follows: $(D_{max} + D_{per})/2$. CTR is the maximum diameter (S_{max}) measured on solid window (window level, − 160HU and window width, 2HU): $CTR = S_{max}/D_{max} \times 100\%$. The mean CT value was measured using the region of interest on the maximum transverse axis of GGN on the lung window, avoiding the trachea, blood vessels, and air-containing cavities as much as possible, and taking the mean value of three measurements as the mean CT value.

Two chest imaging diagnosticians with > 15 years of working experience independently analyzed the images without knowing the clinical data and pathological diagnosis of the patients. Any inconsistent results were solved after discussion.

Statistical analysis

When comparing the LPA and n-LPA groups, two independent sample *t* tests were used to assess continuous variables, including age, mean CT diameter, mean CT value, and CTR. Categorical variables were analyzed using the Pearson chi-square test and Fisher's exact test, including sex, smoking history, and HRCT features. The binary logistic regression analysis was performed on continuous and categorical variables with statistical significance in the univariate analysis. A simple logistic regression model was created using the backward elimination process. The receiver operating characteristic (ROC) analysis was performed using the logistic regression model, and continuous variables with statistical significance were identified in multivariate analysis. The area under the curve (AUC) was used to evaluate the discrimination efficiency of the model in the LPA and n-LPA groups. The cutoff value was defined as the maximum value of the Youden's index. All univariable and multivariate analyses were performed using IBM SPSS version 21.0 software. A *P*-value of < 0.05 was considered statistically significant.

Results

Clinical data and continuous variable analysis

Among 589 patients, 203 were men and 386 were women (average age, 55.03 ± 10.07 years; range, 23–78 years); of these patients, 122 were smokers, 462 were nonsmokers, and five had an unknown smoking history. A total of 260 patients underwent one-lobe lobectomy, 269 underwent single-wedge resection or segmental resection, one underwent two-lobe lobectomy (right upper lobe + middle lobe), 25 underwent one-lobe lobectomy combined with one-segmental or wedge resection, and 31 with two lesions and three with three lesions underwent segmental or wedge resection. Furthermore, 77 patients underwent multiple GGN resections, including 32 patients with two nodules, three with three nodules, and one with four nodules.

Among 630 GGNs, 367 were included in the LPA and 263 in the n-LPA groups (among them, 221 were acinar-predominant type, 28 were papillary-predominant type, three were solid-predominant type, and 11 were micropapillary-predominant type) (Fig. 2). The mean diameter, mean CT value, and CTR were significantly smaller in the LPA group than in the n-LPA group (14.49 vs. 15.43 mm, $P = 0.021$; −566.1 HU vs. −449.3 HU, $P < 0.001$; 9.1% vs. 16.3%, $P < 0.001$) (Table 2). No significant difference was found in sex, age, and smoking history between the LPA and n-LPA groups ($P = 0.522$, 0.663, and 0.396, respectively) (Table 1).

Table 1
Clinical data analysis of GGN

Clinical information	Total number of patients (n = 589)	Number of GGNs (n = 630)		*P*
		LPA(367)	n-LPA(263)	
Age (year), mean ± standard deviation	55.03 ± 10.07	54.91 ± 9.82	55.26 ± 10.19	0.663
Sex				0.522
Male	203 (34.5%)	129 (35.1%)	86 (32.7%)	
Female	386 (65.5%)	238 (64.9%)	177 (67.3%)	
Smoking history (5 missing cases)				0.396
No	462 (79.1%)	293 (80.7%)	205 (77.9%)	
Yes	122 (20.9%)	70 (19.3%)	58 (22.1%)	

GGN: ground-glass nodule; LPA: lepidic-predominant adenocarcinoma; n-LPA: nonlepidic-predominant adenocarcinoma. $P < 0.05$ was considered statistically significant.

Table 2
High-resolution computed tomography features of ground-glass nodules

Features	Classification	LPA (367)	n-LPA (263)	*P*
Mean diameter (mm), mean ± standard deviation		14.49 ± 5.22	15.43 ± 4.79	0.021
Mean CT value (HU), mean ± standard deviation		−566.1 ± 98.2	−449.3 ± 111.5	< 0.001
CTR(%), mean ± standard deviation		9.1 ± 15.5	16.3 ± 19.5	< 0.001
Location	RUL	146 (39.8%)	95 (36.1%)	0.477
	RML	29 (7.9%)	17 (6.5%)	
	RLL	52 (14.2%)	45 (17.1%)	
	LUL	95 (25.9%)	64 (24.3%)	
	LLL	45 (12.3%)	42 (16.0%)	
Type	pGGN	262 (71.4%)	149 (56.7%)	< 0.001
	mGGN	105 (28.6%)	114 (43.3%)	
Deep lobulation	No	148 (40.3%)	35 (13.3%)	< 0.001
	Yes	219 (59.7%)	228 (86.7%)	
Spiculation	No	280 (76.3%)	101 (38.4%)	< 0.001
	Yes	87 (23.7%)	162 (61.6%)	
Vascular change	No	206 (56.1%)	53 (20.2%)	< 0.001
	Yes	161 (43.9%)	210 (79.8%)	
Bronchial change	No	92 (25.1%)	40 (15.2%)	0.003
	Yes	275 (74.9%)	223 (84.8%)	
Bubble-like lucency	No	314 (85.6%)	218 (82.9%)	0.374
	Yes	53 (14.4%)	45 (17.1%)	
Pleural indentation sign	No	178 (48.5%)	120 (45.6%)	0.518
	Yes	189 (51.5%)	143 (54.4%)	
Tumor–lung interface	Unclear	122 (33.2%)	46 (17.5%)	< 0.001
	Clear	245 (66.8%)	217 (82.5%)	

LPA, lepidic-predominant adenocarcinoma; n-LPA, nonlepidic-predominant adenocarcinoma; CTR, consolidation-to-tumor ratio; pGGN, pure ground-glass nodule; mGGN, mixed ground-glass nodule; RUL, right upper lobe; RML, right middle lobe; RLL. right lower lobe; LUL, left upper lobe; LLL, left lower lobe. $P < 0.05$ was considered statistically significant.

Analyzing HRCT features of GGN

The location of GGN was as follows: 241 in the right upper lobe, 46 in the middle lobe, 97 in the lower lobe, 159 in the left upper lobe, and 87 in the left lower lobe. No significant difference was observed in the GGN location, bubble-like lucency, and pleural indentation sign between the LPA and n-LPA groups (P = 0.477, 0.374, and 0.518, respectively). The frequencies of mGGN, deep lobulation, spiculation, vascular change, bronchial change, and clear tumor–lung interface were significantly lower in the LPA group than in the n-LPA group (*P* < 0.001, < 0.001, < 0.001, < 0.001, = 0003, and < 0.001, respectively) (Table 2).

Binary logistic regression analysis of GGN

Binary logistic regression analysis was performed on HRCT features with statistical significance in univariate analysis, including mean diameter, mean CT value, CTR, deep lobulation, spiculation, vascular change, bronchial change, and tumor–lung interface. As nodule types were strongly associated with CTR, nodule types were excluded from logistic regression analysis. Binary logistic regression analysis showed that high CT value [P < 0.001; odds ratio (OR) = 1.009], deep lobulation (P < 0.001; OR = 0.279), spiculation (P < 0.001; OR = 0.470), vascular change (P = 0.034; OR = 0.636), and bronchial change (P = 0.046; OR = 0.592) were independent predictors of increasing the risk of the n-LPA group, whereas small CTR (P = 0.007; 0.982) was a factor that reduced the risk of the n-LPA group (Table 3).

Table 3
Ability to distinguish IPA between the LPA group and n-LPA group using the backward elimination process of binary logistic regression

Feature	B	SE	*P* value	OR	95% CI
Mean CT value	0.009	0.001	< 0.001	1.009	1.007, 1.011
CTR	-0.018	0.007	0.007	0.982	0.969, 0.995
Deep lobulation	1.179	0.257	< 0.001	3.250	1.962, 5.382
Spiculation	0.667	0.216	0.002	1.949	1.275, 2.977
Vascular change	0.944	0.231	< 0.001	2.571	1.636, 4.041
Bronchial change	0.557	0.265	0.036	1.745	1.037, 2.935
Constant	2.346	0.660	< 0.001	10.441	

LPA, lepidic-predominant adenocarcinoma; n-LPA, nonlepidic-predominant adenocarcinoma; CTR, consolidation-to-tumor ratio; SE, standard error; OR, odds ratio (OR > 1 indicates the risk factor of n-LPA; OR < 1 indicates the protective factors of n-LPA). *P* < 0.05 was considered statistically significant.

Logistic regression model performance and ROC curve analysis

ROC analysis was performed on the mean CT value, CTR, and logistic regression model with significant differences in multivariate analysis, which showed that the AUC was 0.781 [95% confidence interval (CI)

0.744–0.818], 0.593 (95% CI: 0.547–0.639), and 0.840 (95% CI: 0.787–0.854), respectively. The optimal cutoff values of the mean CT and CTR were − 472.5 HU (sensitivity, 60.5%; specificity, 83.1%) and 27.4% (sensitivity, 38.4%; specificity, 83.9%), respectively. The sensitivity and specificity of logistic regression model were 76.4% and 78.7%, respectively (Table 4). Logistic regression model combined with mean CT value, CTR, and morphological HRCT features had significantly higher predictive effect than that using only mean CT value or CTR ($P < 0.001$) (Fig. 3).

Table 4
Comparison of the mean CT value, CTR, and ROC curve of the logistic regression model to distinguish IPA between the n-LPA and LPA groups

Factor	AUC value (95% confidence interval)	Cutoff value	Sensitivity (%)	Specificity (%)	*P*
Mean CT value	0.781(0.744–0.818)	-472.5	60.5%	83.1%	< 0.001
CTR	0.593(0.547–0.639)	27.4%	38.4%%	83.9%	< 0.001
Logistic model	0.840(0.808–0.871)	3.958	76.4%	78.7%	< 0.001

Cutoff value: The cutoff value of ROC curve of logistic regression model is the factor value or predictive probability value of the model and the maximum value of Youden's index. LPA, lepidic-predominant adenocarcinoma; n-LPA, nonlepidic-predominant adenocarcinoma; CTR, consolidation-to-tumor ratio; AUC, area under the curve. $P < 0.05$ was considered statistically significant.

Discussion

In univariate analysis, significant differences were observed in the nodule type, deep lobulation, spiculation, tumor–lung interface, vascular change, bronchial change, mean diameter, mean CT value, and CTR between the LPA and n-LPA groups ($P < 0.05$). Multivariate analysis showed that the mean CT value and CTR were higher in the n-LPA group than in the LPA group. HRCT features such as deep lobulation, spiculation, vascular change, and bronchial change supported n-LPA. The AUC for identifying LPA and n-LPA by logistic regression model was 0.840 (95% CI: 0.787–0.854), and the sensitivity and specificity were 76.4% and 78.7%, respectively.

In previous studies [17–19] comparing IPA with preinvasive lesions, the CT value of GGN pulmonary adenocarcinoma was confirmed to be associated with invasiveness. The larger the CT value, the stronger the tumor invasiveness. Eguchi et al. [17] demonstrated that in pGGN, lesions with CT values of > − 680HU were more likely to be IPAs. Zhou et al. [20] showed that lesions with CT values of > − 583.6HU and > − 571.6HU in pGGN and mGGN, respectively, were more likely to be IPAs. In mGGN, studies [21–23] also showed that the solid component represented the fibroblast proliferation or invasive tumor component. Therefore, we can reasonably infer that the larger the mean CT value of the GGN, the greater the proportion of the solid, and the greater the possibility of nonlepidic IPA with more invasive

components. Our study also confirmed that a mean CT value of > − 472.5HU and a CTR of > 27.4% were more likely to be seen in nonlepidic IPA.

A large number of previous studies [5, 8, 15, 24, 25] have shown that marginal lobulation and spiculation on GGN are predictive features of malignant lesions. Zhang et al. [26] classified the bronchus of GGN into three types: type I, with intact bronchial lumen; type II, with dilated or tortuous bronchial lumen; and type III, with bronchial obstruction. A total of 85 among 231 patients with IPAs had types II and III, suggesting that bronchial change is a predictor of invasiveness. Gao et al. [27] divided the relationship between GGN and blood vessels into four types: type I, vessels passed by GGN without detectable supplying branches to the lesions; type II, vessels passed through the lesions without obvious morphological changes in traveling path or size; type III, vessels within lesions were tortuous or rigid without an increase in amount; and type IV, more complex vascular changes than the other types, such as irregular expansion and convergence of multiple blood vessels. Among 74 IPAs with GGN, 38 showed types III and IV vascular changes, indicating that they were more prone to invasive behavior. Liang et al. [23] also demonstrated that the number of blood vessels in GGN is a risk factor for predicting invasiveness; other studies [28, 29] also demonstrated that the growth and metabolism of invasive tumor tissues accelerated, the required nutrients increased, and then angiogenesis factors in the tumor increased, which consequently increased new tumor blood vessels. In this study, the frequencies of deep lobulation, spiculation, and bronchial and vascular changes were high, suggesting n-LPA with strong invasiveness, which is consistent with the above reports. Histologically, the typical feature of adenocarcinoma is fibroblastic interstitial infiltration [25]. With increased invasiveness, the fibrous tissue was proliferative. In addition to the collapse and shrinkage of the pulmonary reticular structure in the lesion and traction of peripheral tissues, lobulation and speculation was observed, which could cause vascular aggregation, displacement, bronchiectasis, and bronchial distortion. The deep lobulation sign may be related to different degrees of tumor cell differentiation and growth rate in all directions. Our study also found that AUC values of the mean CT values and CTR of GGN were 0.840 (sensitivity, 76.4%, specificity, 78.7%), 0.781 (sensitivity, 60.5%, specificity, 83.1%), and 0.593 (sensitivity, 38.4%, specificity, 83.9%), respectively. The logistic regression model was obtained by combining HRCT features, the mean CT values and CTR .Therefore, we believe that the HRCT features of GGN, including deep lobulation, spiculation, vascular change, and bronchial change, can improve the sensitivity, which is better than the use of the mean CT value or CTR alone in distinguishing LPA from n-LPA. Differentiating LPA and n-LPA is very important for the preoperative planning of surgical procedures and simultaneously as a reference value for GGN management. For GGN in patients with deep lobulation and vascular and bronchial changes, the follow-up should be terminated and surgical treatment should be considered.

In univariate analysis, a fuzzy tumor–lung interface was more likely to occur in the LPA group than in the n-LPA group. Considering that the main growth mode in the LPA group was that the tumor cells adhered to the wall along the alveolar septum and the arrangement was relatively loose, air in the alveolar cavity was increased, the invasive region was relatively small, and the CT spatial resolution was limited; when the CT value of the edge part with more air content is close to that of adjacent normal lung tissue, the tumor–lung interface of GGN on CT is fuzzy [30]. Hwang et al. [31] showed that in patients with early

pulmonary adenocarcinoma measuring < 3 cm, disease-free survival was remarkably correlated with the size of the solid part of the tumor, but not with the whole tumor. In this study, the data of the mean GGN diameter significantly overlapped (14.49 ± 5.22 vs. 15.43 ± 4.79), and no significant difference was observed in multivariate analysis. This may be related to the choice of T1 invasive adenocarcinoma in this group, which is also consistent with the above-described results. Takashima et al. [24] confirmed that the incidence of pleural indentation sign increased with increased tumor invasiveness. Masahiro et al. [32] found that the volume ratio of solid components in GGN was > 63% and that the incidence of pleural indentation sign increased. Nevertheless, we investigated GGN with CTR of < 50% and did not consider the distance between the nodules and pleura; therefore, pleural indentation sign was not statistically significant between the two groups.

This study has certain limitations. First, this was a retrospective analysis, mainly based on pathological diagnosis. The assessment of IPA subtypes may be inconsistent, especially when multiple subtype components coexisted. Second, this study only focused on lepidic and nonlepidic types of IPA and did not further analyze imaging differences among other nonlepidic subtypes.

Conclusions

The appearance of HRCT features, including deep lobulation, spiculation, vascular changes, and bronchial changes, possibly indicates nonlepidic IPA in GGN, and the diagnosis of lepidic IPA is supported when the mean CT value is < − 472.5 HU or CTR is < 27.4%. Simultaneously, the combined application of mean CT value, CTR, and HRCT features can effectively improve the efficiency of differential diagnosis.

Declarations

Acknowledgements

Not applicable.

Authors’ contributions

PZ and TL: Conceptualization, formal analysis, visualization, writing original draft, and editing. SZ: Conceptualization, supervision, project administration, and review. XT and XJ: Data curation, investigation, review and editing. SZ had full access to all the data in the study and take responsibility for the integrity of the data and the accuracy of the data analysis. All authors have read and approved the final version of manuscript.

Funding

This study was supported by the National Natural Science Foundation of China (81641068) and the Clinical Research Support Fund of PLA General Hospital (2016FC-TSYS-1040).

Availability of data and materials

The dataset used and/or analyzed during the current study are available from corresponding author on reasonable request.

Ethics approval and consent to participate

The study was approved by theEthics Committee of Fourth Medical Center of Chinese PLA General Hospital (approval No. 2019YL002-HS001). Written informed consent was obtained from all study participants.

Consent for publication

Not applicable.

Competing interests

The authors have declared that they have no conflicts of interests.

References

[1] Stang A, Schuler M, Kowall B, et al. Lung Cancer Screening Using Low Dose CT Scanning in Germany. Extrapolation of results from the National Lung Screening Trial. Dtsch Arztebl Int. 2015;112:637-44.

[2] Matsuguma H, Mori K, Nakahara R, et al. Characteristics of subsolid pulmonary nodules showing growth during follow-up with CT scanning. Chest. 2013;143:436-43.

[3] Naidich DP, Bankier AA, MacMahon H, et al. Recommendations for the management of subsolid pulmonary nodules detected at CT: a statement from the Fleischner Society. Radiology. 2013;266:304-17.

[4] Horeweg N, Rosmalen JV, Heuvelmans MA, et al. Lung cancer probability in patients with CT-detected pulmonary nodules: a prespecified analysis of data from the NELSON trial of low-dose CT screening. Lancet Oncol. 2014;15:1332-41.

[5] MacMahon H, Naidich DP, Goo JM, et al. Guidelines for Management of Incidental Pulmonary Nodules Detected on CT Images: From the Fleischner Society 2017. Radiology. 2017;284:228-43.

[6] Matsunaga T, Suzuki K, Takamochi K, et al. What is the radiological definition of part-solid tumour in lung cancer? Eur J Cardiothorac Surg. 2017;51:242-7.

[7] Travis WD, Brambilla E, Nicholson AG, et al. The 2015 World Health Organization Classification of Lung Tumors: Impact of Genetic, Clinical and Radiologic Advances Since the 2004 Classification. J Thorac Oncol. 2015;10:1243-60.

[8] Lee HY, Jeong JY, Lee KS, et al. Solitary pulmonary nodular lung adenocarcinoma: correlation of histopathologic scoring and patient survival with imaging biomarkers. Radiology. 2012;264:884-93.

[9] Yoshizawa A, Motoi N, Riely GJ, et al. Impact of proposed IASLC/ATS/ERS classification of lung adenocarcinoma: prognostic subgroups and implications for further revision of staging based on analysis of 514 stage I cases. Mod Pathol. 2011;24:653-664.

[10] Naso JR, Wang G, Pender A, et al. Intratumoral Heterogeneity in PD-L1 Immunoreactivity is Associated with Variation in Non-Small Cell Lung Carcinoma Histotype. Histopathology. 2020;76:394-403.

[11] Jiang G, Chen C, Zhu Y, et al.[Shanghai Pulmonary Hospital Experts Consensus on the Management of Ground-Glass Nodules Suspected as Lung Adenocarcinoma (Version 1)]. Zhongguo Fei Ai Za Zhi. 2018;21:147-59.

[12] Moon Y, Lee KY, Moon SW, et al. Sublobar Resection Margin Width Does Not Affect Recurrence of Clinical N0 Non-small Cell Lung Cancer Presenting as GGO-Predominant Nodule of 3 cm or Less. World J Surg. 2017;41:472-9.

[13] Feng SH, Yang ST. The new 8th TNM staging system of lung cancer and its potential imaging interpretation pitfalls and limitations with CT image demonstrations. Diagn Interv Radiol. 2019;25:270-9.

[14] Ye T, Deng L, Wang S, et al. Lung Adenocarcinomas Manifesting as Radiological Part-Solid Nodules Define a Special Clinical Subtype. J Thorac Oncol. 2019;4:617-7.

[15] Jin X, Zhao SH, Gao J, et al. CT characteristics and pathological implications of early stage (T1N0M0) lung adenocarcinoma with pure ground-glass opacity. Eur Radiol. 201;25:2532-40.

[16] Hotta T, Tsubata Y, Tanino A, et al. Comparative postoperative outcomes of GGN-dominant vs single lesion lung adenocarcinomas. J Cardiothorac Surg. 2020;15:149.

[17] Eguchi T, Yoshizawa A, Kawakami S, et al. Tumor size and computed tomography attenuation of pulmonary pure ground-glass nodules are useful for predicting pathological invasiveness. PLoS One. 2014;9:e97867.

[18] Liang J, Xu XQ, Xu H, et al. Using the CT features to differentiate invasive pulmonary adenocarcinoma from pre-invasive lesion appearing as pure or mixed ground-glass nodules. Br J Radiol. 2015;88:20140811.

[19] Lee HY, Choi YL, Lee KS, et al. Pure ground-glass opacity neoplastic lung nodules: histopathology, imaging, and management. AJR Am J Roentgenol. 2014;202:W224-3.

[20] Zhou QJ, Zheng ZC, Zhu YQ, et al. Tumor invasiveness defined by IASLC/ATS/ERS classification of ground-glass nodules can be predicted by quantitative CT parameters. J Thorac Dis. 2017;9:1190-200.

[21] Park CM, Goo JM, Lee HJ, et al. Nodular ground-glass opacity at thin-section CT: histologic correlation and evaluation of change at follow-up. Radiographics. 2007;27:391-408.

[22] Lee HJ, Goo JM, Lee CH, et al. Nodular ground-glass opacities on thin-section CT: size change during follow-up and pathological results. Korean J Radiol. 2007;8:22-31.

[23] Soda H, Nakamura Y, Nakatomi K, et al. Stepwise progression from ground-glass opacity towards invasive adenocarcinoma: long-term follow-up of radiological findings. Lung Cancer. 2008;60:298-301.

[24] Takashima S, Maruyama Y, Hasegawa M, et al. CT findings and progression of small peripheral lung neoplasms having a replacement growth pattern. AJR Am J Roentgenol.

2003;180:817-26.

[25] Lee HJ, Goo JM, Lee CH, et al. Predictive CT findings of malignancy in ground-glass nodules on thin-section chest CT: the effects on radiologist performance. Eur Radiol.

2009;19:552-60.

[26] Zhang Y, Qiang JW, Shen Y, et al. Using air bronchograms on multi-detector CT to predict the invasiveness of small lung adenocarcinoma. Eur J Radiol. 2016;85:571-7.

[27] Gao F, Li M, Ge X, et al. Multi-detector spiral CT study of the relationships between pulmonary ground-glass nodules and blood vessels. Eur Radiol. 2013;23:3271-7.

[28] Lee HY, Lee KS. Ground-glass opacity nodules: histopathology, imaging evaluation, and clinical implications. J Thorac Imaging. 2011;26:106-18.

[29] Fontanini G, Vignati S, Boldrini L, et al. Vascular endothelial growth factor is associated with neovascularization and influences progression of non-small cell lung carcinoma. Clin Cancer Res. 1997;3:861-5.

[30] Borczuk AC, Qian F, Kazeros A, et al. Invasive size is an independent predictor of survival in pulmonary adenocarcinoma. Am J Surg Pathol. 2009;33:462-9.

[31] Hwang EJ, Park CM, Ryu Y, et al. Pulmonary adenocarcinomas appearing as part-solid ground-glass nodules: is measuring solid component size a better prognostic indicator? Eur Radiol. 2015;25:558-67.

[32] Yanagawa M, Tanaka Y, Leung AN, et al. Prognostic importance of volumetric measurements in stage I lung adenocarcinoma. Radiology. 2014;272:557-67.

Figures

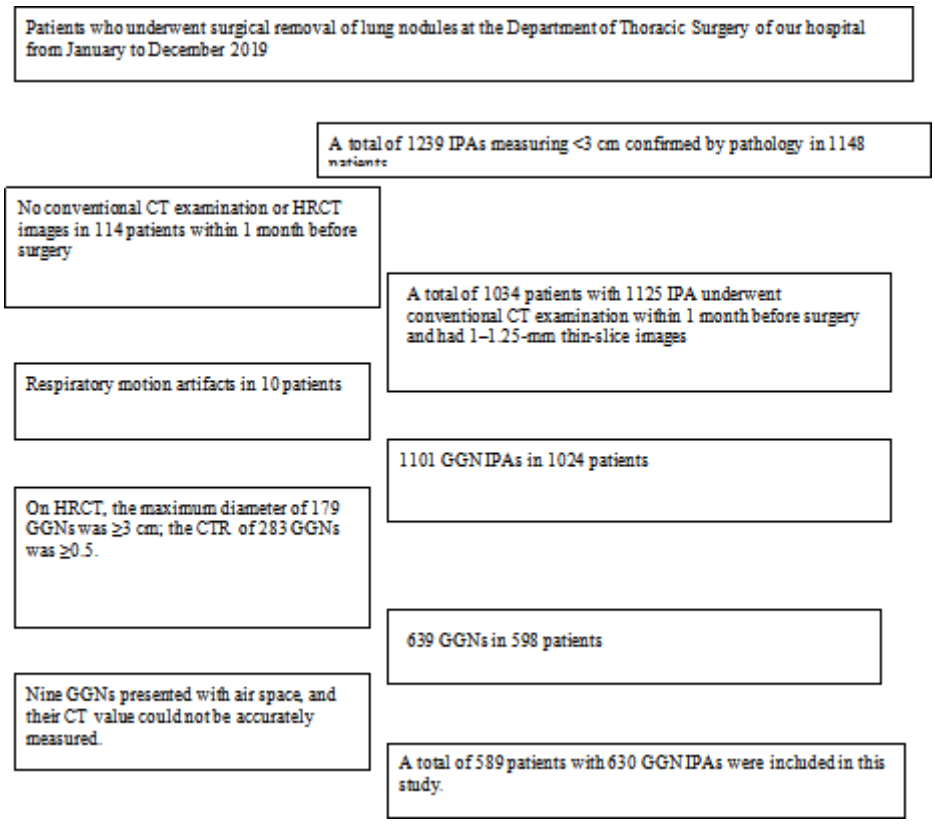

Figure 1

Flow chart of patient screening. HRCT, high-resolution computed tomography; IPA, invasive pulmonary adenocarcinoma; GGN, ground-glass nodule; CTR, consolidation-to-tumor ratio.

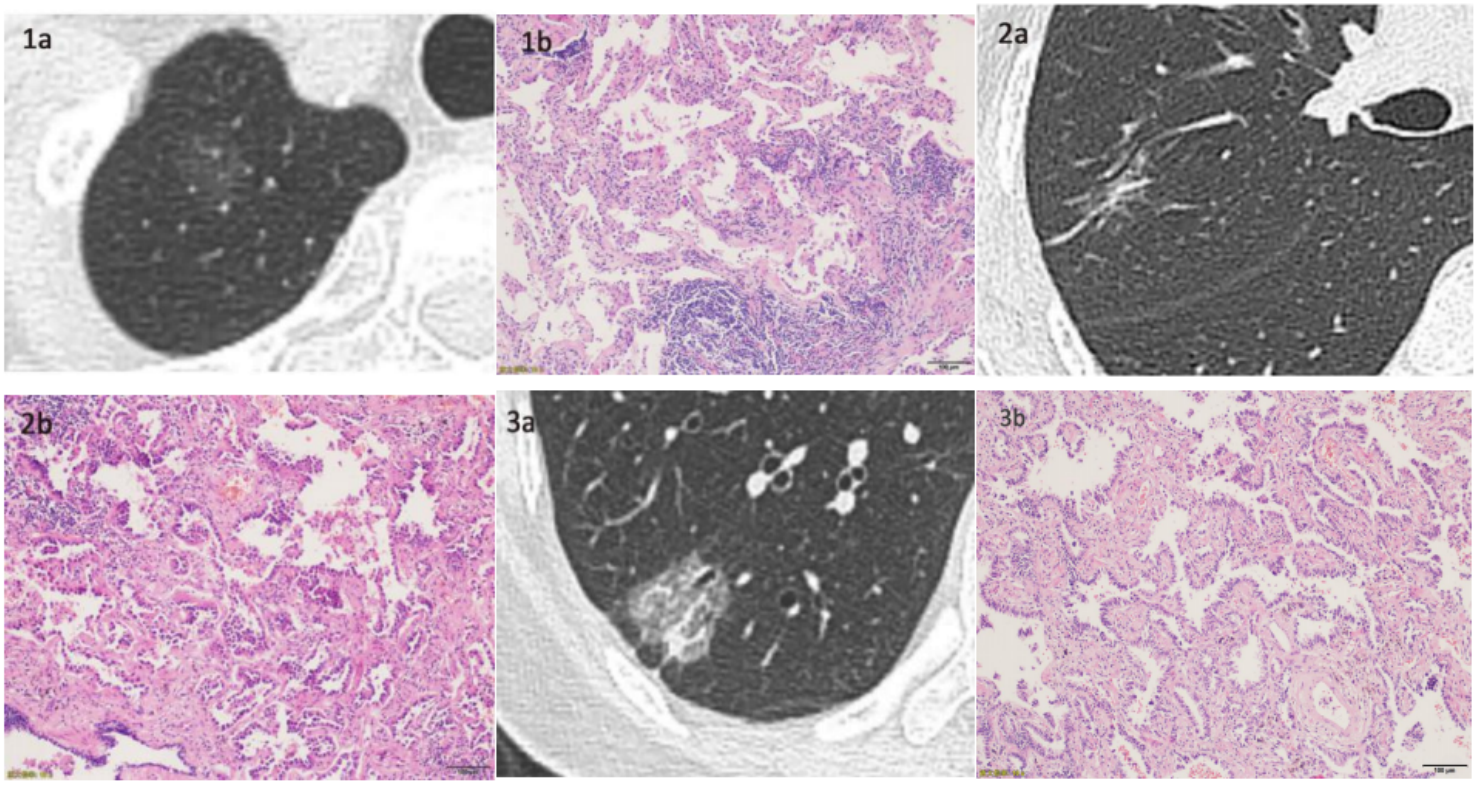

Figure 2

CT and pathological characteristics of GGN. (1a) A 72-year-old female patient with lepidic-predominant adenocarcinoma. HRCT lung window shows pGGN of the right upper lobe, without lobulation at the edge, spiculation, and vascular or bronchial changes and with unclear tumor–lung interface. (1b) The pathological image of the same patient (HE × 100) shows lepidic tumor cells, with unilateral boot nail like arrangement, alveolar septum thickening, infiltrating part in the lower right corner, and no vascular or bronchial changes found. (2a) A 51-year-old female patient had acinar-predominant adenocarcinoma. HRCT lung window showed pGGN in the upper lobe of the right lung, lobulated spiculation at the edge, pleural indentation sign, and vascular and bronchial changes. (2b) The pathological image of the same patient (HE × 100) shows that tumor cells were mainly acinar-like growth, interstitial fiber hyperplasia, and air bronchogram found in the lower left corner. (3a) A 55-year-old female patient had papillary-predominant adenocarcinoma. HRCT lung window shows mGGN in the right lower lobe, lobulated spiculation at the edge, pleural indentation sign, and bronchial and vascular changes. (3b) The pathological image of the same patient (HE × 100) shows that the tumor tissue was mainly papillary growth. Interstitial fibers and tumor cells were observed outside the blood vessels in the lower right corner. HRCT, high-resolution computed tomography; HE, hematoxylin and eosin; pGGN, pure ground-glass nodule; mGGN, mixed ground-glass nodule.

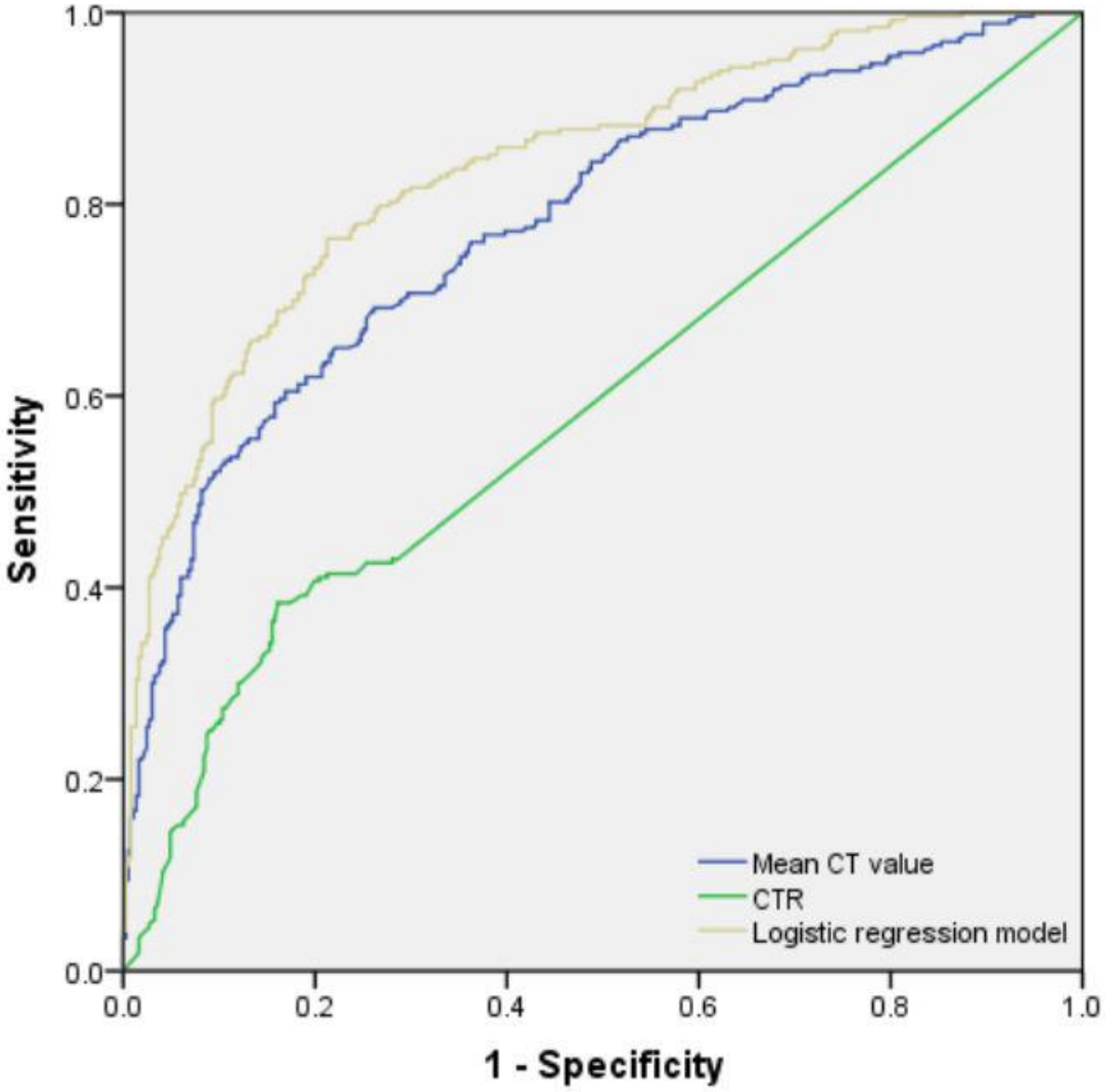

Figure 3

Ability of the mean CT value, CTR, and logistic regression model to distinguish LPA from n-LPA. Logistic regression model includes mean CT value, CTR, deep lobulation, spiculation, vascular change, and bronchial change. The AUC value (AUC = 0.840) was significantly higher than the mean CT value (AUC = 0.781) or CTR (AUC = 0.593), and the diagonal line represents the reference line.